


PLZF and its fusion proteins are pomalidomide-dependent CRBN neosubstrates

Nobuyuki Shimizu¹, Tomoko Asatsuma-Okumura ¹, Junichi Yamamoto², Yuki Yamaguchi², Hiroshi Handa ¹✉ & Takumi Ito ¹✉

Pomalidomide and lenalidomide are immunomodulatory agents that were derived from thalidomide. Cereblon (CRBN) is a common direct target of thalidomide and related compounds and works as a Cullin Ring 4 E3 ubiquitin ligase (CRL4) with DDB1, CUL4, and ROC1. The substrate specificity of CRL4^{CRBN} is modulated by thalidomide-related compounds. While lenalidomide is approved for the treatment of several diseases including multiple myeloma, 5q- syndrome, mantle cell lymphoma, and follicular lymphoma, pomalidomide is approved only for the treatment of lenalidomide-resistant multiple myeloma. Here we show that PLZF/ZBTB16 and its fusion proteins are pomalidomide-dependent neosubstrates of CRL4^{CRBN}. *PLZF* joins to *RARα* or potentially other partner genes, and the translocation causes leukemias, such as acute promyelocytic leukemia and T-cell acute lymphoblastic leukemia. We demonstrate that pomalidomide treatment induces PLZF-*RARα* degradation, resulting in antiproliferation of leukemic cells expressing PLZF-*RARα*. This study highlights a potential therapeutic role of pomalidomide as a degrader of leukemogenic fusion proteins.

¹Department of Chemical Biology, Tokyo Medical University, 6-1-1, Shinjuku, Shinjuku-ku, Tokyo 160-8402, Japan. ²School of Life Science and Technology, Tokyo Institute of Technology, Yokohama 226-8501, Japan. ✉email: handa@tokyo-med.ac.jp; takumii@tokyo-med.ac.jp

Pomalidomide and lenalidomide are thalidomide derivatives developed as immunomodulatory compounds in the mid-1990s¹. Pomalidomide has an additional amino group attached to a phthaloyl ring of thalidomide, whereas lenalidomide lacks one carbonyl group of pomalidomide. These compounds have been shown to be up to 50,000 times more potent at inhibiting TNF- α production than the parental compound, with pomalidomide being around 10 times more potent than lenalidomide². These drugs have been shown to possess potent anti-myeloma activity. Multiple myeloma is a B-cell malignancy and known as a refractory disease. Pomalidomide and lenalidomide are effective in the treatment of multiple myeloma and other types of blood cancer^{3,4}.

Pomalidomide, lenalidomide, and thalidomide have a common primary target, CRBN, a substrate receptor of CRL4 E3 ligase that is complexed with DDB1, Cul4, and Roc1⁵. CRBN is a 441- or 442-amino-acid ubiquitously expressed protein that is evolutionally conserved from plants to humans⁵. When a thalidomide-related compound binds to CRBN, neosubstrates are recruited to CRBN and ubiquitinated for proteasomal degradation⁶. Various drug-dependent neosubstrates are recruited to CRBN in a cell type- and/or compound-specific manners. In multiple myeloma cells, pomalidomide and lenalidomide induce the breakdown of Ikaros (IKZF1) and Aiolos (IKZF3), resulting in IRF4 downregulation and cell growth defects^{7–9}. Thalidomide also degrades Ikaros and Aiolos, although less effective¹⁰. Pomalidomide also induces degradation of ARID2, a subunit of the chromatin remodeling complex PBAF and thereby exerts anti-myeloma effect¹¹. In developing embryos, thalidomide induces the degradation of Δ Np63 α and TAp63 α , gene products of *TP63*, and thereby causes limb and ear defects, respectively¹². In embryonic stem (ES) cells and induced pluripotent stem (iPS) cells, thalidomide, pomalidomide, and lenalidomide induce the degradation of SALL4, which might also be involved in thalidomide teratogenicity^{13–15}. In myelodysplastic syndrome 5q- cells, lenalidomide, but not pomalidomide or thalidomide, induces degradation of casein kinase 1 α (CK1 α), a critical regulator of 5q- cell growth, through CRL4^{CRBN}¹⁰. In acute myeloid leukemia cells, CC-885, but no other CRBN-binding drugs, drives the breakdown of the translation termination factor GSPT1, resulting in antiproliferation¹⁶. Several 3D structures of CRBN-drug-neosubstrate complexes have been determined^{16–19}. CRBN-binding drugs work as molecular glues²⁰ connecting CRBN with neosubstrates; different neosubstrates can be recruited by different drugs, particularly due to the difference in phthaloyl moiety. For example, the lack of a carbonyl group of lenalidomide avoids steric clash, allowing for binding of CRBN to CK1 α ¹⁷. The extended chloro-methyl phenyl group and urea structure of CC-885 contribute to the interaction between CRBN and GSPT1¹⁶. The amino group of lenalidomide and pomalidomide binds to a critical glutamine residue of Ikaros and Aiolos and enhances their interactions with CRBN¹⁸. Most of the neosubstrates identified so far have at least one β -hairpin motif containing a specific glycine that is critical for their interactions with CRBN^{16–18}.

Among approved CRBN-binding drugs, lenalidomide is currently widely used for not only multiple myeloma but also MDS 5q-syndrome²¹, mantle cell lymphoma²², and follicular lymphoma²³. However, pomalidomide is limited to relapsed or refractory multiple myeloma²⁴. To expand the clinical use of pomalidomide, we investigated “neosubstrate-based” drug repositioning, which employs the function of neosubstrates to consider therapeutic applications of the drug. We screened pomalidomide-specific neosubstrates associated with diseases from various tissues to find out the therapeutic effects of pomalidomide.

Here we show that zinc finger and BTB domain containing 16 (ZBTB16)/promyelocytic leukemia zinc finger (PLZF) is a pomalidomide-specific neosubstrate. *PLZF* undergoes chromosomal

translocations to cause leukemias such as acute promyelocytic leukemia (APL) and T-cell acute lymphoblastic leukemia (T-ALL). A fusion protein composed of PLZF and Retinoic Acid Receptor A (RAR α) is associated with a rare type of APL and has been well characterized²⁵. Moreover, a fusion gene comprising *PLZF* and *ABL1* is found in some patients with T-ALL²⁶. We demonstrate that pomalidomide drives proteasomal degradation of PLZF-RAR α through CRL4^{CRBN} at pharmacologically relevant concentrations, resulting in antiproliferation of leukemic cells. Moreover, we show that PLZF-ABL1 is also downregulated by pomalidomide. This study highlights a therapeutic role of pomalidomide in certain types of leukemia.

Results

PLZF is a pomalidomide-dependent CRBN-binding protein.

We first sought to identify pomalidomide-dependent CRBN-binding proteins from various cell extracts. The CRL4^{CRBN} complex was purified using anti-FLAG agarose from 293T cells stably expressing FLAG-HA (FH)-CRBN. Then, purified CRL4^{CRBN} was incubated with another cell extract in the presence or absence of pomalidomide for coimmunoprecipitation using anti-HA agarose beads. From long-term neuroepithelial stem (lt-NES) cell extracts, several pomalidomide-dependent CRBN-binding proteins were identified by LC/MS, such as ZBTB16/PLZF, methionine-tRNA ligase, guanosine monophosphate synthetase, and several metabolic enzymes (Supplementary Fig. 1a–c and Supplementary Data 1). PLZF is a 673-amino-acid, C2H2-type zinc finger (ZF)-containing transcription factor. Since many of the known neosubstrates of CRL4^{CRBN} contain a β -hairpin motif flanked by a C2H2-type ZF motif^{18,27}, we hypothesized that PLZF would serve as a neosubstrate of CRL4^{CRBN}.

To confirm the pomalidomide-dependent interaction between CRBN and PLZF, Myc-FLAG (MF)-tagged PLZF was ectopically expressed in 293T expressing FH-CRBN. Immunoprecipitation using anti-HA antibody showed that CRBN binds to PLZF only in the presence of pomalidomide (Fig. 1a). We confirmed this interaction by coimmunoprecipitating endogenous CRBN and PLZF from lt-NES cell extracts (Supplementary Fig. 2a). In vitro binding assay using GST-fused CRBN and FLAG-tagged PLZF also confirmed pomalidomide-dependent binding of CRBN to PLZF (Fig. 1b and Supplementary Fig. 2b). The interaction was increased by pomalidomide in a dose-dependent manner, but not by thalidomide or lenalidomide substantially (Fig. 1b).

PLZF is a pomalidomide-dependent neosubstrate of CRBN.

We next investigated whether pomalidomide affects the PLZF protein level at pharmacologically relevant concentrations. lt-NES cells were treated with pomalidomide, lenalidomide, or thalidomide at 10 μ M for 24 h (Fig. 1c). Pomalidomide, but not thalidomide or lenalidomide, markedly decreased the PLZF protein level, while all the compounds decreased SALL4, a previously reported neosubstrate (Fig. 1c). Time-course analysis showed that pomalidomide substantially decreases the PLZF protein level in 3 h (Supplementary Fig. 2c, d). The peak plasma concentrations of these compounds are \sim 5.4 μ M (thalidomide), \sim 2 μ M (lenalidomide), and 0.2 μ M (pomalidomide)²⁸. Concordantly, pomalidomide decreased the PLZF protein level by more than 50% at 0.1 μ M (Fig. 1d, e), suggesting that pomalidomide affects PLZF expression in vivo. Immunofluorescence analysis confirmed the decrease of PLZF by pomalidomide in living cells (Fig. 1f, g). The decrease of PLZF by pomalidomide was confirmed by using other cell lines such as human neural stem cell line Sai2 and human acute myeloid leukemia cell line KG1 (Supplementary Fig. 2e–g). By using genome editing, we established lt-NES cells lacking the *CRBN* gene. Pomalidomide did not affect the PLZF protein level in

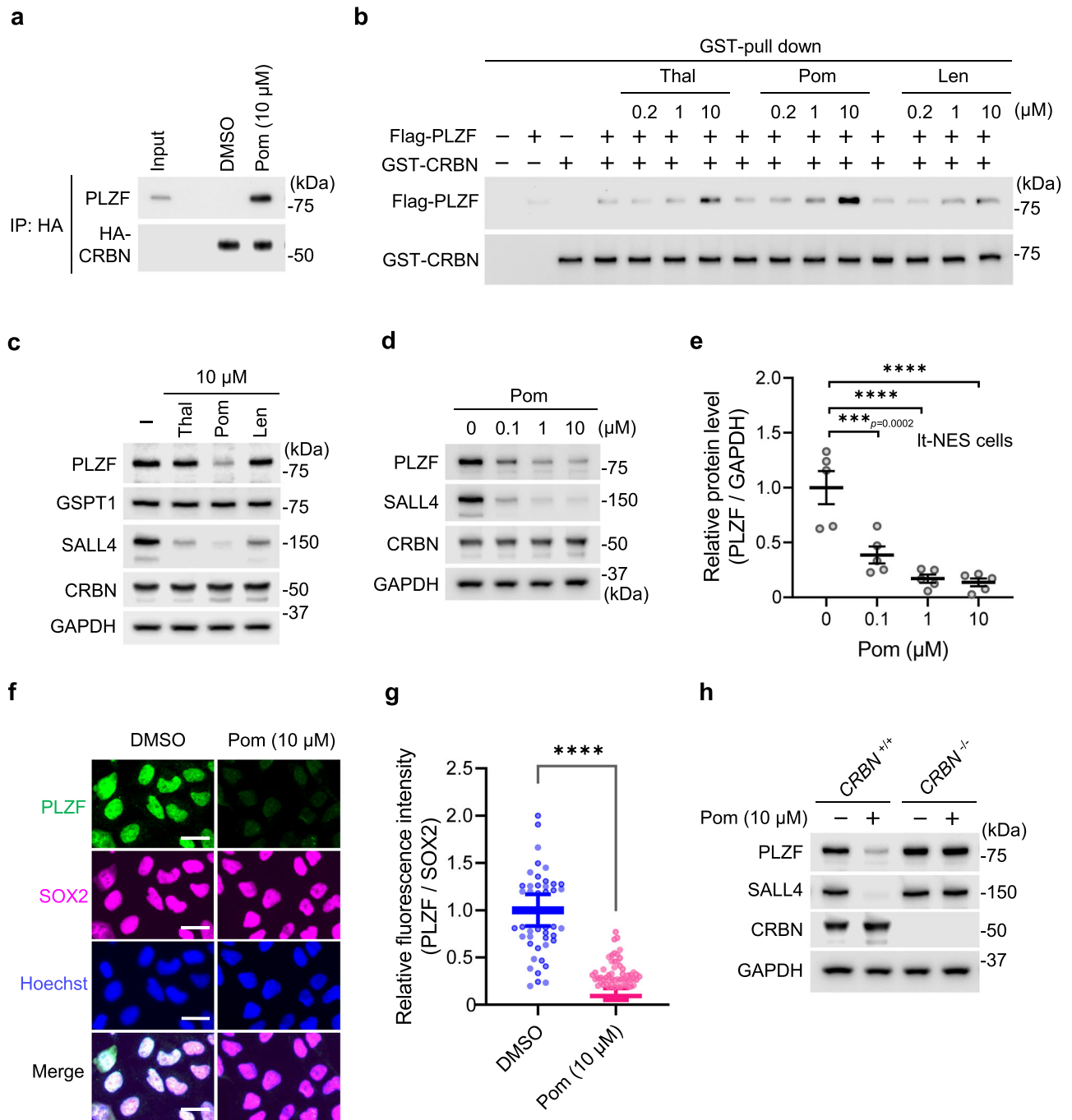


Fig. 1 PLZF is a downstream target of the CRBN-pomalidomide pathway. **a** The CRL4^{CRBN} complex containing FH-CRBN was incubated with Lt-NES extracts and then subjected to immunoblotting with the indicated antibodies. **b** The interaction between purified recombinant GST-CRBN and PLZF in the presence of the indicated compounds was analyzed by immunoblotting. **c, d** Lt-NES cells were incubated with DMSO or one of the indicated compounds at the indicated concentrations for 24 h and harvested for immunoblot analysis. **e** The immunoblots shown in **d** were quantified, and relative intensities of PLZF/GAPDH were calculated and normalized to the control value (DMSO). Data are shown as mean \pm SEM from five biologically independent samples from two independent experiments. $***p < 0.001$, $****p < 0.0001$, one-way ANOVA with multiple comparisons test. **f** Immunofluorescence staining of PLZF (green), SOX2 (magenta), and Hoechst (blue) in Lt-NES cells treated with DMSO or 10 μ M pomalidomide. Merge represents the stacked images of PLZF, SOX2, and Hoechst. Scale bar, 20 μ m. **g** From the immunofluorescence data in **f**, relative intensities of PLZF/SOX2 were calculated and normalized to the control value (DMSO). Data are shown as mean \pm SEM from three biologically independent samples ($n = 434$ for DMSO and $n = 405$ for 10 μ M pomalidomide treatment). $****p < 0.0001$, two-sided Mann-Whitney U -test. **h** The PLZF protein levels in parental and CRBN^{-/-} Lt-NES cells were analyzed by immunoblotting. All experiments were conducted more than twice independently, and representative data sets are shown.

CRBN-deficient cells (Fig. 1h), demonstrating that CRBN is required for pomalidomide-induced downregulation of PLZF.

To investigate whether PLZF is a neosubstrate of CRL4^{CRBN}, Lt-NES cells were co-treated with pomalidomide and MLN4924, a

neddylation inhibitor. As expected, the decrease of PLZF was reversed by MLN4924 (Fig. 2a), pointing to the involvement of a Cullin-based E3 ligase. In addition, cycloheximide treatment showed that the protein half-life of PLZF was shortened by

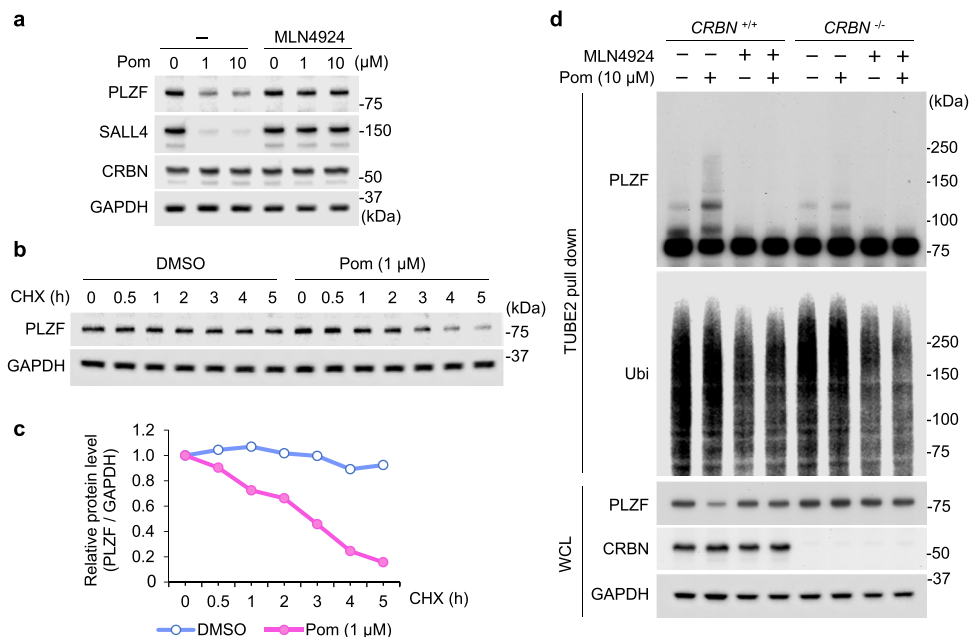


Fig. 2 PLZF is a pomalidomide-specific neosubstrate of CRL4^{CRBN}. **a** Lt-NES cells were incubated with DMSO or pomalidomide at the indicated concentration for 6 h and harvested for immunoblot analysis. Cells were pretreated with DMSO or 1 μ M MLN4924. **b** Immunoblot analysis of Lt-NES cells treated with 100 μ g/mL CHX and DMSO or 1 μ M pomalidomide for the indicated periods. **c** PLZF protein levels in **b** were quantified, and relative intensities of PLZF/GAPDH are shown. **d** Wild-type or *CRBN*^{-/-} cells were treated with 10 μ M pomalidomide and/or 1 μ M MLN4924 for 7 h and subjected to affinity purification of ubiquitinated proteins using TUBE2 agarose beads. WCL whole-cell lysate. All experiments were conducted more than three times with similar results.

pomalidomide (Fig. 2b, c and Supplementary Fig. 3a, b) whereas its mRNA level was unaffected by pomalidomide (Supplementary Fig. 3c). Furthermore, the cellular ubiquitination status of PLZF was examined in the presence or absence of CRBN-binding drugs. PLZF ubiquitination was induced by pomalidomide, but not by thalidomide or lenalidomide substantially (Fig. 2d and Supplementary Fig. 3d). Under the same conditions, SALL4 ubiquitination was induced by all the CRBN-binding drugs tested (Supplementary Fig. 3d). In *CRBN*-deficient cells, pomalidomide-induced ubiquitination of PLZF was not observed (Fig. 2d). Lastly, *in vitro* ubiquitination assay showed that PLZF is directly polyubiquitinated by CRL4^{CRBN} in the presence of corresponding E1 and E2 enzymes and ATP in a pomalidomide-inducible manner (Supplementary Fig. 3e). These results led us to conclude that PLZF is a pomalidomide-dependent neosubstrate of CRL4^{CRBN}.

Identification of two structural degrons in PLZF. PLZF is composed of the N-terminal BTB-POZ domain and nine C2H2-type ZF motifs (Fig. 3a)²⁹. Recent reports have shown that many ZF-containing neosubstrates of CRBN have a CXXCG sequence motif(s) as the structural degron (X denotes any amino acid) and that the glycine residue is critical for their interactions with CRBN (Fig. 3b)^{16–18,27}. Sequence analysis of PLZF found that six out of the nine ZFs possess a putative degron. We, therefore, constructed two PLZF mutants whose three glycine residues are replaced with alanine. While PLZF^{G496/552/580A} was coimmunoprecipitated with CRBN in a pomalidomide-dependent manner as efficiently as wild-type PLZF, PLZF^{G410/438/467A} lacked CRBN-binding activity (Supplementary Fig. 4a), and its expression was not downregulated by pomalidomide (Supplementary Fig. 4b). Next, single and double point mutants of PLZF were constructed based on the triple point mutant. Although all the single point mutants bound CRBN in a pomalidomide-dependent manner,

PLZF^{G410/467A} did not bind CRBN appreciably (Fig. 3c and Supplementary Fig. 4c), suggesting that both G410 and G467 are critical for CRBN binding. Furthermore, a heterologous system using EGFP fused to a ZF motif of 23 amino acids was employed to validate the above finding (Fig. 3d). Binding experiments revealed that both ZF1 (404–426) and ZF3 (461–483) bind to CRBN in the presence of pomalidomide and the key glycine residue (Fig. 3e), leading us to conclude that PLZF has two structural degrons.

Some of the known neosubstrates of CRBN are resistant to degradation induced by CRBN-binding drugs in mice. Structural studies have shown that V388I substitution in mouse CRBN causes steric clash and prevents its interaction with neosubstrates^{10,16,17}. We examined if pomalidomide induces degradation of PLZF in *CRBN*^{-/-} cells expressing mouse CRBN or human CRBN^{V388I}. As a result, PLZF downregulation was observed in cells expressing human wild-type CRBN but not in cells expressing mouse CRBN or human CRBN^{V388I} (Supplementary Fig. 4d), suggesting that PLZF binds to CRBN with a stereospecificity similar to known neosubstrates containing a CXXCG motif.

Pomalidomide-induced degradation of PLZF fusion proteins. PLZF is a transcription factor involved in multiple biological processes such as neurogenesis, spermatogenesis, invariant natural killer T-cell development, and leukemogenesis^{25,30–32}. PLZF was originally identified as a gene that is fused to *RAR α* following the t(11;17)(q23;q21) translocation in patients with APL (Fig. 4a)³³. PLZF-*RAR α* is associated with a rare subset of APL with a poor prognosis. If pomalidomide induces proteasomal degradation of PLZF-*RAR α* at pharmacologically relevant concentrations, pomalidomide might be useful for the treatment of this type of APL. In addition, a recent study revealed that PLZF is fused with *ABL1* in two patients with T-ALL (C11 and C23)²⁶.

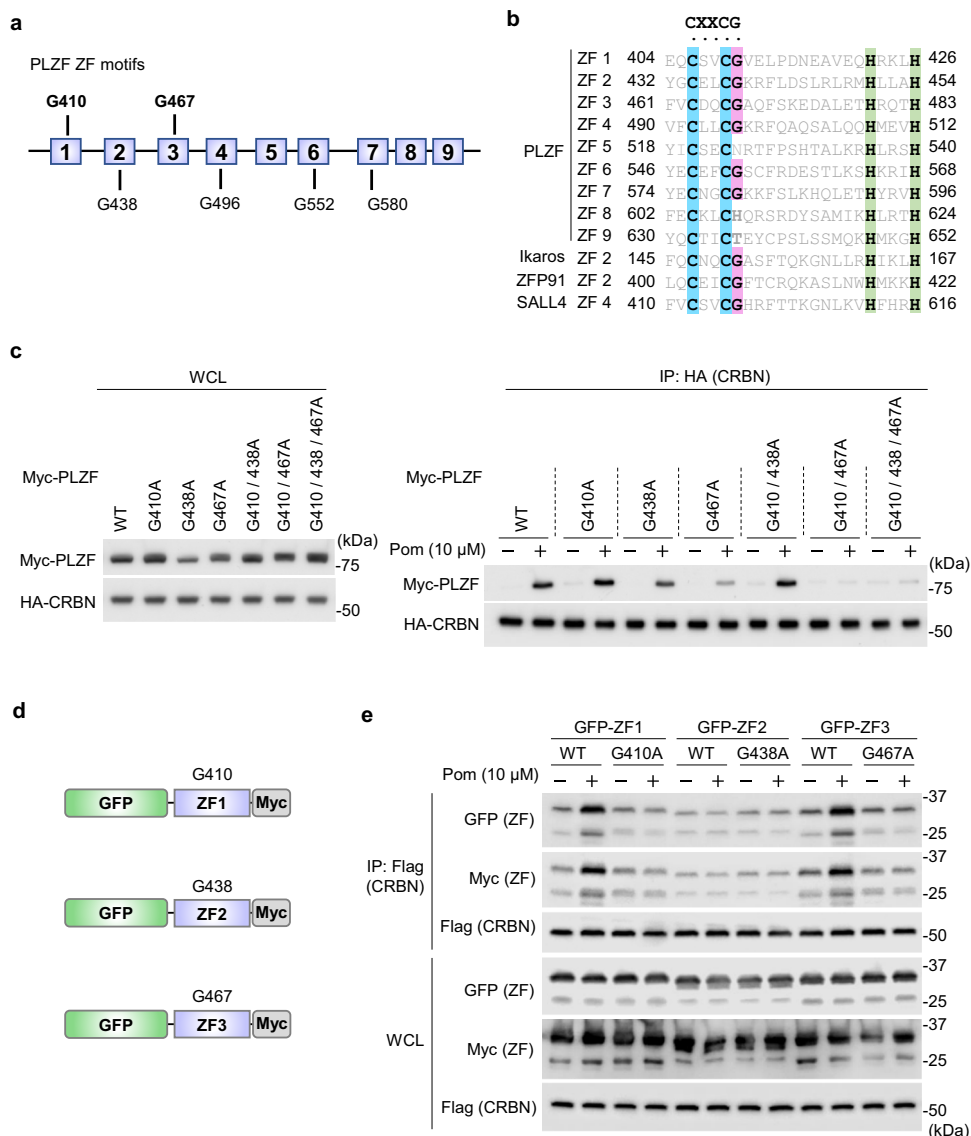


Fig. 3 G410 and G467 of PLZF are critical for its binding to CRBN in the presence of pomalidomide. **a** Schematic representation of the ZF motifs of PLZF. **b** Multiple sequence alignment showing PLZF ZF motifs along with validated ZF degrons from Ikaros, ZFP91, and SALL4. Cys and His residues (blue and green, respectively) comprising ZF motifs and critical Gly residues (red) are highlighted. **c** FLAG-HA (FH)-CRBN and Myc-FLAG (MF)-PLZF carrying point mutations were coexpressed in 293T cells and immunoprecipitated with anti-HA antibody in the presence or absence of pomalidomide. **d** Schematic representation of EGFP-fused PLZF ZF proteins. **e** FH-CRBN and EGFP-fused PLZF ZF proteins were coexpressed in 293T cells and immunoprecipitated with anti-Flag antibody in the presence or absence of pomalidomide. WCL whole-cell lysate. All experiments were conducted more than twice with similar results.

In all the cases identified so far, the N-terminal region of PLZF containing the first few ZF motifs is fused with partner gene products and plays a critical role in leukemogenesis (Fig. 4a). First, we investigated the stability of PLZF-RARα in the presence of pomalidomide. The PLZF-RARα protein level was decreased by 0.2 μM pomalidomide in 293T cells overexpressing PLZF-RARα, but not in the corresponding cells lacking CRBN (Fig. 4b). CRBN coimmunoprecipitated PLZF-RARα in the presence of pomalidomide (Fig. 4c and Supplementary Fig. 5a). The extent to which this interaction was stabilized by thalidomide or lenalidomide was weak, as observed for the CRBN-PLZF interaction (Supplementary Fig. 5a). Moreover, the mutational analysis showed that PLZF-RARα binding to CRBN is abolished by G410A mutation in ZF1, but not by G438A mutation in ZF2 (Fig. 4d), suggesting that PLZF-RARα binds to CRBN only through PLZF’s ZF1.

We also investigated the stability of PLZF-ABL1 and its interaction with CRBN in the presence or absence of pomalidomide. T-ALL cases C23 and C11 possess slightly different translocation breakpoints, resulting in the PLZF-ABL1 chimeric proteins retaining the first two or three zinc fingers of PLZF, respectively (Fig. 4a). CRBN coimmunoprecipitated the two PLZF-ABL1 isoforms at a comparable level in the presence of pomalidomide (Fig. 4e). Moreover, the PLZF-ABL1 protein levels, overexpressed in 293T cells, were reduced by pomalidomide treatment (Supplementary Fig. 5b), indicating that PLZF-ABL1 also serves as a pomalidomide-dependent neosubstrate of CRBN.

Antiproliferative effect of pomalidomide on cells expressing PLZF-RARα. Next, we employed B412, a U937-derived stable clone with zinc-inducible expression of PLZF-RARα, which has

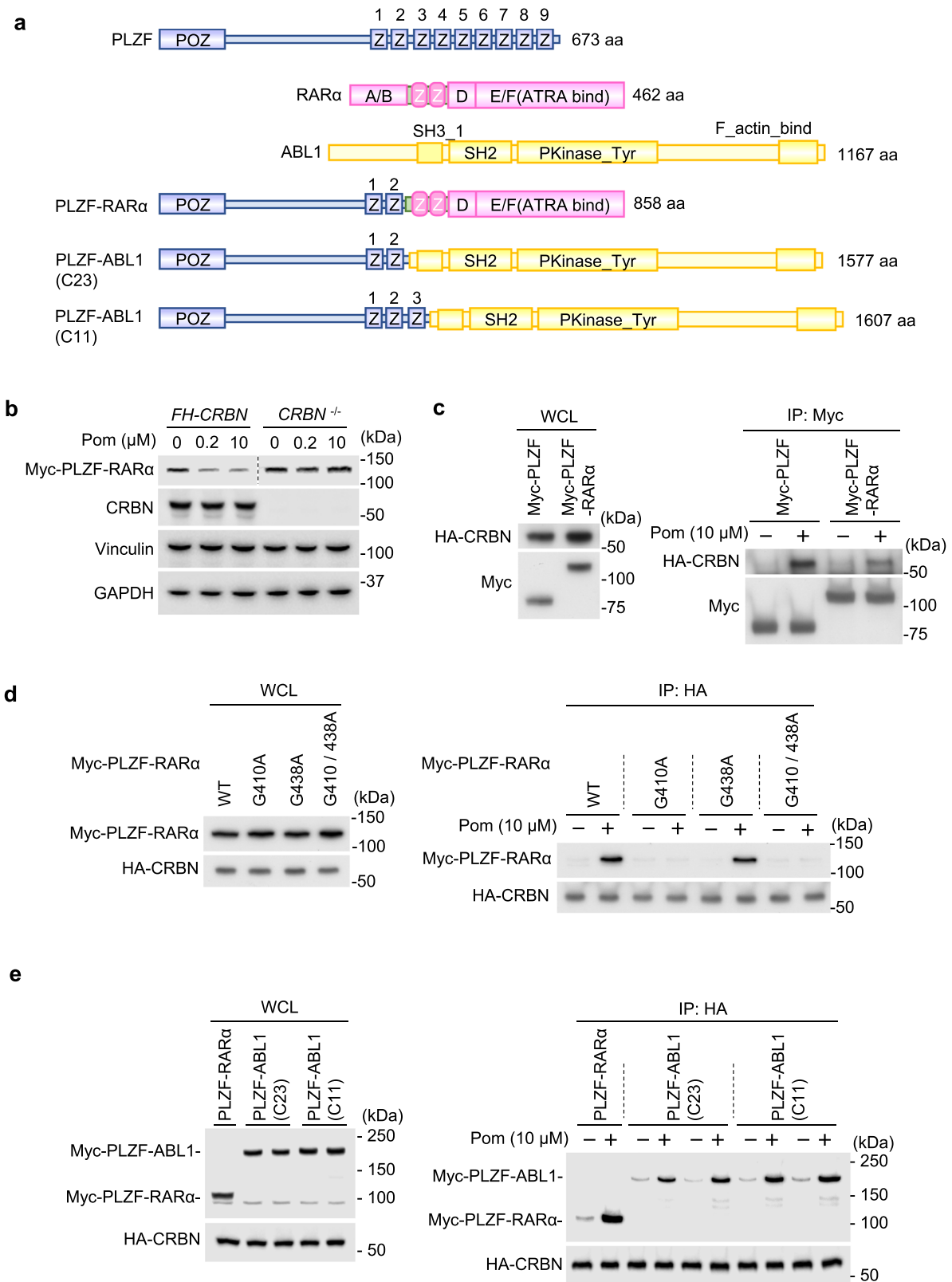


Fig. 4 PLZF fusion proteins are neosubstrates of CRL4^{CRBN}. **a** Schematic representation of PLZF, RAR α , ABL1, and three PLZF fusion proteins. **b** Myc tagged-PLZF-RAR α was overexpressed in 293T expressing FLAG-HA (FH)-CRBN and 293T lacking CRBN, treated with DMSO or pomalidomide, and subjected to immunoblot analysis. **c** FH-CRBN and Myc-FLAG (MF)-PLZF or Myc-PLZF-RAR α were coexpressed in 293T cells and immunoprecipitated with anti-Myc antibody in the presence or absence of pomalidomide. **d** FH-CRBN and Myc-PLZF-RAR α carrying point mutations were coexpressed in 293T cells and immunoprecipitated with anti-HA antibody in the presence or absence of pomalidomide. **e** FH-CRBN and Myc-PLZF-ABL1 were coexpressed and immunoprecipitated in the presence or absence of pomalidomide. WCL whole-cell lysate. All experiments were conducted more than twice with similar results.

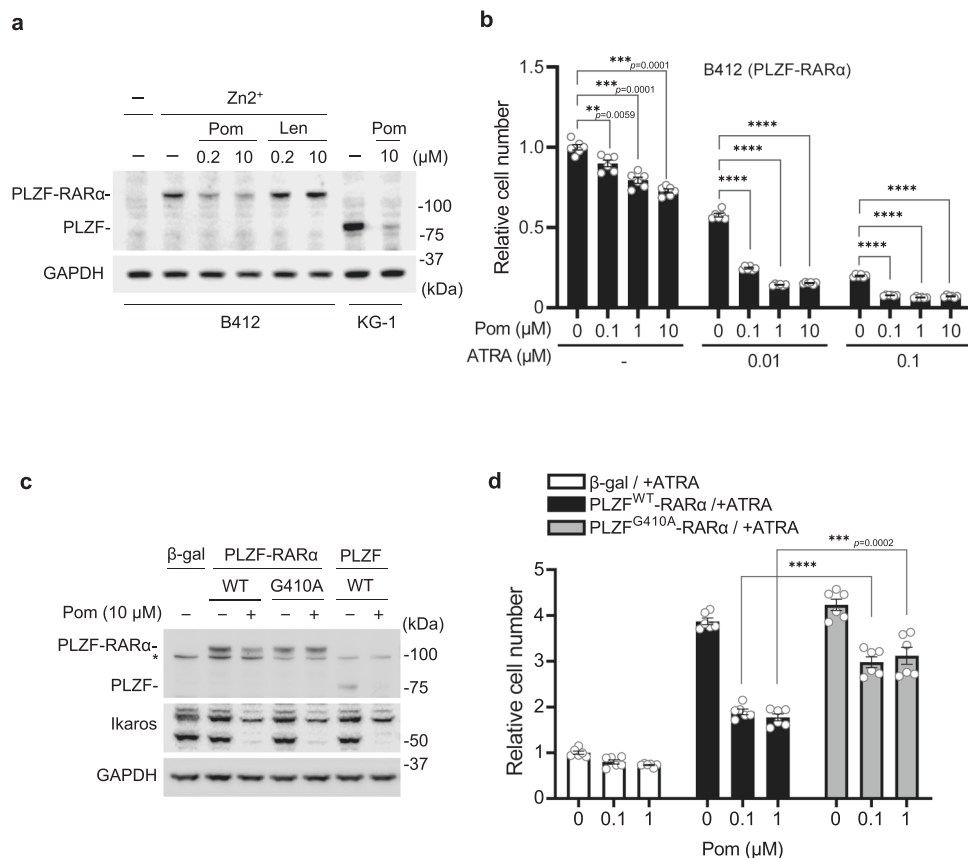


Fig. 5 Antiproliferative effect of pomalidomide on cells expressing PLZF-RARα. **a** B412 and KG-1 cells were treated with lenalidomide or pomalidomide for 48 h. Where indicated, 100 μM ZnSO₄ (Zn²⁺) was added 6 h prior to drug treatment. Cells were harvested and analyzed by immunoblotting. **b** The effect of pomalidomide on the proliferation of B412 cells. To B412 cells induced to express PLZF-RARα by ZnSO₄, pomalidomide and ATRA were added 6 days prior to cell counting. Data are shown as mean ± SEM from six biologically independent samples. ***p* < 0.01; ****p* < 0.001; *****p* < 0.0001. Statistical significance was calculated with a two-way ANOVA with multiple comparisons test. **c** U937 cells expressing the indicated constructs were treated with pomalidomide or left untreated for 24 h, harvested, and subjected to immunoblotting. Asterisk denotes nonspecific signal. **d** U937 cells expressing the indicated constructs were treated with ATRA and the indicated concentrations of pomalidomide for 7 days prior to cell counting. Data are shown as mean ± SEM from six biologically independent experiments. ****p* < 0.001; *****p* < 0.0001. Statistical significance was calculated with two-way ANOVA with multiple comparisons test. Experiments were conducted more than twice with similar results.

been used as a cell line model of PLZF-RARα-positive APL in many studies^{34–36}. Zinc-induced PLZF-RARα expression in B412 cells was downregulated by pomalidomide, but not by lenalidomide (Fig. 5a and Supplementary Fig. 5c). To investigate whether pomalidomide exerts its antiproliferative effect through the degradation of PLZF-RARα, B412 cells were treated with pomalidomide, all-*trans* retinoic acid (ATRA), or both for 6 days and subjected to tetrazolium-based assays for cell viability. ATRA alone inhibited B412 cell growth in a concentration-dependent manner (Fig. 5b). Pomalidomide alone also showed a modest inhibitory effect. Remarkably, in the presence of a suboptimal concentration of ATRA, pomalidomide showed a more prominent inhibitory effect at pharmacologically relevant concentrations (Fig. 5b). This finding led us to investigate whether ATRA influences the interaction between CRBN and PLZF-RARα. In fact, however, ATRA had little effect on their interaction (Supplementary Fig. 5d), suggesting that ATRA and pomalidomide exert their antiproliferative effects by distinct mechanisms.

To determine whether the antiproliferative effect of pomalidomide on B412 cells is mediated by CRBN binding to ZF1 of PLZF-RARα, U937 cells constitutively expressing PLZF^{WT}-RARα, PLZF^{G410A}-RARα, PLZF^{WT}, or control β-galactosidase were established by using a lentiviral vector. While PLZF^{WT}-RARα, PLZF^{G410A}-RARα, and PLZF^{WT} were expressed at a

similar level in the absence of pomalidomide, only PLZF^{WT}-RARα and PLZF^{WT} were substantially downregulated by pomalidomide (Fig. 5c). Forced expression of PLZF^{WT}-RARα or PLZF^{G410A}-RARα resulted in an approximately four-fold increase in cell number after 7 days of incubation (Fig. 5d), demonstrating the growth-promoting activity of the fusion protein. The growth-promoting activity of PLZF^{G410A}-RARα was not efficiently reversed by pomalidomide, whereas that of PLZF^{WT}-RARα was reversed by pomalidomide (Fig. 5d), indicating that CRBN binding to PLZF-RARα and its destruction is responsible for the antiproliferative effect of pomalidomide.

Discussion

This study illustrates that PLZF and its fusion proteins are pomalidomide-dependent neosubstrates of CRL4^{CRBN}. PLZF is susceptible to proteasomal degradation in the presence of pomalidomide, but not in the presence of thalidomide or lenalidomide. PLZF possesses two degrons in ZF1 (404–426) and ZF3 (461–483). PLZF-RARα and PLZF-ABL1, fusion proteins associated with APL and T-ALL, respectively, are eliminated by pomalidomide at pharmacologically relevant concentrations. In addition, pomalidomide exerts an antiproliferative effect on U937 cells expressing PLZF-RARα.

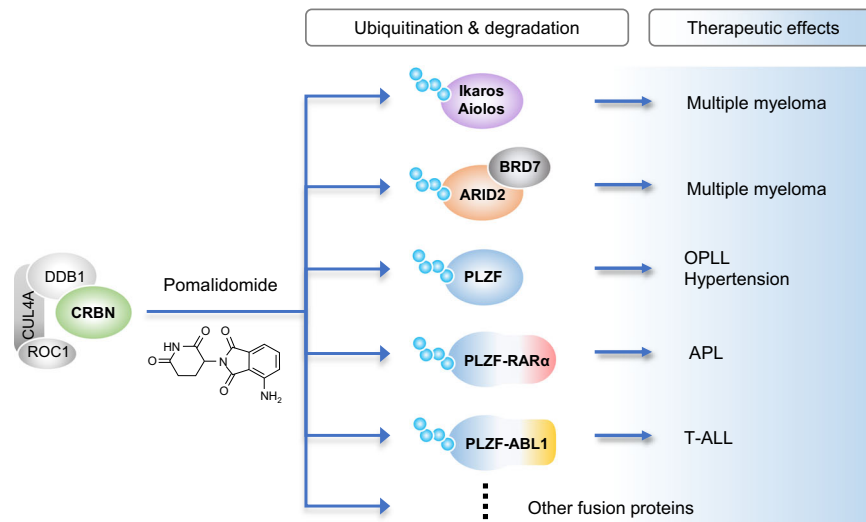


Fig. 6 Schematic representation of pomalidomide effects. In multiple myeloma, pomalidomide induces the degradation of Ikaros, Aiolos, and ARID2, resulting in anti-myeloma effects. Pomalidomide also induces degradation of PLZF and may exert several physiological and pathological effects via its breakdown. In APL and T-ALL expressing PLZF fusion proteins, pomalidomide may exert an anti-cancer effect by inducing the degradation of the leukemogenic fusion proteins.

APL is characterized by excessive proliferation of immature leukemic cells harboring chromosomal translocations between *RARα* and one of several partner genes²⁵. The vast majority of APL patients bear *PML-RARα* and respond to ATRA therapy. On the other hand, APL patients bearing *PLZF-RARα* are resistant to ATRA-induced differentiation and have poor prognosis^{25,37}. Given the growth-promoting activity of *PLZF-RARα*³⁵, targeted degradation of *PLZF-RARα* is a promising therapeutic approach against refractory APL carrying *PLZF-RARα*. Our data have shown that pomalidomide, an immunomodulatory drug approved for the treatment of multiple myeloma, is an attractive candidate for a *PLZF-RARα* degrader (Fig. 6).

PROTACs or molecular glue degraders targeting *PLZF* may also be useful for the treatment of other diseases. One such example is ossification of the posterior longitudinal ligament (OPLL), a disease-causing cervical myopathy that is characterized by ectopic bone formation in the paravertebral ligament^{38,39}. A previous study reported that *PLZF* is up-regulated in OPLL cells and that knockdown of *PLZF* leads to downregulation of osteoblast-specific genes and inhibition of osteoblastic differentiation³⁹. Concordantly, a following study showed that *PLZF* is recruited to the enhancers of osteogenic genes and activates nearby genes through epigenetic regulation⁴⁰. Thus, pomalidomide may exert therapeutic effects on OPLL via degradation of *PLZF* (Fig. 6). Other studies have shown that *PLZF* is associated with metabolic and cardiac traits of spontaneously hypertensive rats (SHRs)^{41–43}. SHR is one of the most widely used model of essential hypertension, which likely develops left ventricular hypertrophy, myocardial fibrosis, and metabolic disturbances. Previous studies have shown that *PLZF* mediates cardiac hypertrophic signaling and that its downregulation ameliorates the metabolic and cardiac traits of the animals^{41,43}. Thus, pomalidomide or other PROTACs targeting *PLZF* using pomalidomide or its derivatives may also be useful for the treatment of metabolic syndrome and cardiovascular diseases (Fig. 6).

During the preparation of this paper, one report independently revealed that *PLZF* is a neosubstrate involved in thalidomide teratogenicity⁴⁴. Using a human transcription factor protein array, the authors identified *PLZF* as a neosubstrate whose degradation is induced by thalidomide and its derivatives.

Meanwhile, here we investigated potential repositioning of thalidomide analogs to leukemias associated with *PLZF* translocation. Thus, these two studies are completely different beyond the identification of *PLZF* as a neosubstrate for *CUL4^{CRBN}*. According to Yamanaka et al.⁴⁴, pomalidomide is most potent in inducing the degradation of *PLZF* among approved thalidomide-based compounds, followed by lenalidomide and thalidomide. In our hands, while pomalidomide is most potent, the efficacy of thalidomide and lenalidomide is very low, if not nonexistent (Fig. 1c and Supplementary Fig. 2e). This is a minor conflict between the two studies. Drug concentration and incubation time were almost the same, but different cell lines were used by the two studies. Thus, a possible explanation for the apparent discrepancy is that the cell lines used in these studies had different ubiquitin-proteasome system activity.

There are numerous fusion genes driving cancers by translocations. Pharmaceutical drugs that target fusion gene products have been developed. One of the most well-known drugs in this category is imatinib, which targets *BCR-ABL* in chronic myeloid leukemia⁴⁵. While kinases and receptors are comparatively easy to be functionally inactivated by small-molecule compounds and are considered druggable, transcription factors and signal transducers are difficult to be targeted by conventional approaches and are considered undruggable⁴⁶. Recently, however, proteolysis targeting chimeras (PROTACs) and molecular glue degraders⁴⁷ have been investigated as a strategy for drug development. Ikaros and Aiolos, *CRBN* neosubstrates and transcription factors essential for myeloma survival, are conventionally undruggable but are now regarded as promising targets for drug development⁴⁸. Similarly, oncogenic fusion proteins without enzymatic activity can also be targeted by PROTACs or molecular glue degraders. Meanwhile, recent studies using massive parallel sequencing and clinical samples have led to the identification of numerous fusion genes^{26,49}. For example, from T-ALL patients, fusion genes, such as *PLZF-ABL1* and *IKZF1-Notch1*, have been found^{26,50}. Since the *PLZF* moiety of *PLZF-ABL1* and the *IKZF1* moiety of *IKZF1-Notch1* carry a structural degraon for *CUL4^{CRBN}*, we speculate that pomalidomide and lenalidomide may also be effective for the treatment of T-ALL carrying these fusion proteins. Thus, PROTAC-based degraders targeting proteins that are frequently mutated and fused to other proteins by chromosomal

translocations may serve as small-molecule drugs for treating multiple diseases caused by common genetic aberrations. At least the approved drug pomalidomide is worth investigating for use in PLZF-associated APL and T-ALL. This study highlights a potential therapeutic use of pomalidomide for the treatment of cancers carrying neosubstrate-fused oncogenic drivers (Fig. 6).

Methods

Cell culture. Human embryonic kidney cell line 293T (ATCC) was maintained in Dulbecco's modified Eagle's medium (Nacalai Tesque) supplemented with 10% fetal bovine serum (Biowest) and Antibiotic-Antimycotic Mixed Stock solution (Nacalai Tesque). Neural stem cell lines AF22 (lt-NES) and Sai2 were cultured on Matrigel (Corning, 354277) and maintained in RHB-A medium (CEL, Y40001) supplemented with 8 μ L/mL Stem Beads FGF2 (Stem Culture Inc, SB500) and 10 ng/mL EGF (PEPROTECH, AF-100). KG1 and U937 cells were maintained in RPMI1640 (ThermoFisher Scientific, A1049101) containing 10% fetal bovine serum. All the cell lines were cultured at 37 °C with 5% CO₂ and were confirmed to be mycoplasma-negative using the MycoAlert Mycoplasma Detection Kit (Lonza).

Reagents. Thalidomide (Toris Biosciences, 0652), pomalidomide (TCI chemicals, 19171-19-8), MLN4924 (Adooq BioScience, 905579-51-3), and all-*trans* retinoic acid (SIGMA, R2625) were purchased from the indicated vendors. Lenalidomide was a kind gift from Celgene.

Plasmids. pCMV6-PLZF-MF and pCMV6-SALL4-MF were purchased from ORIGENE. PLZF-RAR α and PLZF-ABL1 cDNAs were synthesized by Eurofins Genomics and GenScript, respectively, and inserted to pCS2(+) and pLenti6. PLZF and PLZF-RAR α mutants were generated by using PrimeSTAR Mutagenesis Basal Kit (TaKaRa). pcDNA3.1-FH-tagged human CRBN was described previously⁵.

Mass spectrometry. 293T cells expressing FH-CRBN were established by lentiviral transduction. Cells (1×10^8) were collected in 1% Triton lysis buffer (50 mM Tris-HCl pH 8.0, 150 mM NaCl, and 1% Triton X-100) supplemented with protease/phosphatase inhibitor cocktail. The cell lysate was mixed with M2 FLAG agarose (Sigma, A2220) and incubated for 3 h. After washing the beads six times with 1% Triton lysis buffer, bound proteins (CRL4^{FH-CRBN}) were eluted with 0.1 mg/mL FLAG peptide. Lt-NES cells (5×10^8) were extracted using 1% Triton lysis buffer containing protease/phosphatase inhibitor cocktail, and the extracts were combined with the CRL4^{FH-CRBN} complex and 0.1% DMSO or 10 μ M pomalidomide. After 12 h of incubation, the mixture was incubated with Anti-HA-Affinity Matrix beads (Roche, 11815016001) for 3 h. After washing the beads five times with 1% Triton lysis buffer, bound proteins were eluted with sodium dodecyl sulfate (SDS) and subjected to SDS-PAGE following Coomassie Brilliant Blue (CBB) staining. Gels were sliced and sent to Medical ProteoScope Co., Ltd. Tryptic peptides were extracted from the slices and subjected to the Ultimate 3000 RSLCnano liquid chromatography (ThermoFisher Scientific) and the Q Exactive Orbitrap mass spectrometer (ThermoFisher Scientific). Data were analyzed by Proteome Discoverer (ver. 2.2) (ThermoFisher Scientific) and Mascot (Matrix Science).

Coimmunoprecipitation assay. For coimmunoprecipitation analysis of exogenous proteins, N-terminally FH-tagged CRBN and C-terminally MF-tagged PLZF were transfected into 293T cells using Lipofectamine 2000 (ThermoFisher Scientific). Cells were collected and extracted by 1% Triton lysis buffer supplemented with protease/phosphatase inhibitor cocktail 48 h after transfection. Extracts were incubated for 12 h in the presence or absence of pomalidomide or its analogs. The mixture was then incubated with anti-HA affinity matrix beads for 3 h. After washing the beads five times with 1% Triton lysis buffer, bound proteins were eluted with SDS and analyzed by immunoblotting.

For coimmunoprecipitation of endogenous proteins, extracts of Lt-NES cells were incubated with mouse monoclonal anti-CRBN44 antibody, generated against amino acids 1–18 of human CRBN⁵¹, for 24 h in the presence or absence of pomalidomide. The mixture was then incubated with Dynabeads Protein G (Veritas) for 3 h. After washing the beads five times with 1% Triton lysis buffer, bound proteins were eluted with SDS and analyzed by immunoblotting.

CRISPR/Cas9-mediated genome editing. For the generation of Lt-NES CRBN^{-/-} and HEK293T CRBN^{-/-} cells, parental cells were transfected with 2 μ g of spCas9-sgRNA targeting CRBN using Nucleofector kit V (Lonza) and program B-23. After transfection, clonal isolation was conducted. The protein level of CRBN in each cell line was assessed by immunoblotting. CRBN guide RNA sequence used was 5'-GCTGATATGGAAGAATTCATGG-3'.

Immunoblotting. Samples were subjected to 7% or 10% SDS-PAGE (DRC XV PANTERA GEL, NXV-225P) and transferred to PVDF membranes using the

Trans-Blot Turbo Transfer System (Bio-Rad). Membranes were blocked with Bullet Blocking One (Nacalai Tesque) and incubated with primary antibodies overnight, followed by three washes with 0.1% TBST and incubation with secondary antibodies for 45 min. After three final washes, the membranes were incubated with Chemi-Lumi One L (Nacalai Tesque, 07880-54) or Chemi-Lumi One Ultra (Nacalai Tesque, 11644-40) for 2 min and subjected to imaging with FUSION FX (Vilber-Lourmat). Rabbit anti-human CRBN65 mAb (Celgene, San Diego, CA, 1:10000 dilution, Lot# CGN-6-4-5), mouse anti-PLZF mAb (39987, Active Motif, 1:1000 dilution, Lot#05313002), mouse anti-PLZF mAb (sc-28319, Santa Cruz, 1:1000 dilution, Lot#C0618), mouse anti-SALL4 mAb (ab57577, Abcam, 1:1000 dilution, Lot#GR3198290-2), mouse anti-Vinculin mAb (ab18058, Abcam, 1:1000 dilution, Lot#GR207163-1), mouse anti-HA11 mAb (901503, BioLegend, 1:1000 dilution, Lot#b207273), mouse anti-Flag M2 mAb (F1804, SIGMA, 1:1000 dilution, Lot#SLBS3530V), rabbit anti-Myc tag (ab9106, Abcam, 1:1000 dilution), rabbit anti-GSPT1 (ab49878, Abcam, 1:1000 dilution, Lot#GR274469-4), rabbit anti-CK1 α mAb (ab108296, Abcam, 1:1000 dilution, Lot#GR53415-9), and rabbit anti-Ikarsos mAb (ab26083, Abcam, 1:1000 dilution, Lot#GR250435-1), rabbit anti-GFP (ab290, Abcam, 1:1000 dilution, Lot#GR3184825-1) were used as primary antibodies. Anti-mouse IgG, HRP-linked Antibody (#7076, Cell Signaling, 1:10,000 dilution, Lot#25) and anti-rabbit IgG, HRP-linked Antibody (#7074, Cell Signaling, 1:10,000 dilution, Lot#33) were used as secondary antibodies. Mouse anti-GAPDH-mAb-HRP-Direct (M171-7, MBL, 1:5000 dilution, Lot#006), mouse anti-Myc-tag mAb-HRP-Direct (M192-7, MBL, 1:2000 dilution, Lot#006), mouse anti-Ub (P4D1)-mAb-HRP (sc-8017, Santa Cruz, 1:1000 dilution, Lot#A0919), anti-Ub mAb (FK2, ENZO, 1:1000 dilution, Lot#07281715), and rabbit anti-GST-tag pAb-HRP-Direct (PM013-7, MBL, 1:1000 dilution, Lot#005) were also used.

Immunofluorescence microscopy. Lt-NES cells were grown on Matrigel-coated 8-well chamber slides (5732-008, IWAKI) for 24 h and further incubated in the presence of DMSO or 10 μ M pomalidomide for 24 h. Then, the media was discarded, and the wells were washed once with PBS. Cells were fixed with 4% paraformaldehyde in PBS for 20 min, washed three times for 5 min with PBS containing 0.1% Triton X-100, and then blocked for 1 h at room temperature with PBS containing 10% FBS. Anti-PLZF (39987, Active Motif, Lot#05313002) and anti-SOX2 (ab92494, Abcam, Lot#GR30587-10) were diluted at 1:100 with PBS containing 10% FBS (antibody dilution buffer) and incubated overnight. After three-time washes with PBS, Alexa Fluor 488 donkey anti-mouse (Life Technologies) and Alexa Fluor 555 anti-rabbit (Life Technologies) antibodies diluted at 1:500 with antibody dilution buffer were added and incubated for 1 h at room temperature. After three-time washes with PBS, coverslips were mounted onto the slides with Aqueous Mounting Medium (TA-030-FM, ThermoFisher Scientific) containing Hoechst 33258 (ab228550, Abcam). Slides were analyzed by fluorescence microscopy at $\times 20$ using an EVOS Imaging System. Fluorescence intensities were quantified by using ImageJ.

Quantitative RT-PCR analysis. From Lt-NES cells treated with 10 μ M pomalidomide or DMSO, RNA was isolated using Sepasol reagent (Nacalai Tesque) and reverse-transcribed using iScript RT Supermix (Bio-Rad) following the manufacturer's instructions. The following primer sets (Eurofins) were used with SsoAdvanced Universal SYBR Green Supermix (Bio-Rad) and a CFX96 Real-Time PCR System (Bio-Rad) to quantify GAPDH and PLZF mRNA levels. GAPDH, 5'-GGATTGGTCGTATTGGG-3' and 5'-GGAAGATGGTGATGGGATT-3'; PLZF, 5'-CGGGACTTTGTGCGATGTG-3' and 5'-GCGGTGGAAGAGGATCTCAA-3'. Relative mRNA levels were calculated by using the $\Delta\Delta$ CT method.

GST-pulldown assay. For binding experiments with purified proteins, Flag-tagged PLZF (Active Motif) and GST-tagged CRBN (Novus Biologicals) were incubated with 10 μ M thalidomide, pomalidomide, or lenalidomide in binding buffer (25 mM Tris-HCl pH 7.5, 150 mM NaCl, 1 mM EDTA, 10% glycerol, and 1% Triton X-100) containing 0.1 mg/mL BSA. After incubation at 4 °C for 20 h, mixtures were further incubated with glutathione Sepharose beads (GE Healthcare) for 3 h. After washing the beads three times, bound proteins were eluted by SDS and analyzed by immunoblotting.

PLZF protein half-life analysis. Sai2 cells were pretreated with DMSO or 1 μ M pomalidomide for 30 min, followed by the addition of 100 μ g/mL cycloheximide (Nacalai Tesque) to the culture medium. At various time points, cells were collected and subjected to immunoblot analysis.

Cellular ubiquitination assays. To assess endogenous ubiquitination of PLZF and SALL4, 2×10^7 Lt-NES cells were pretreated with DMSO or 1 μ M MLN4924, treated with DMSO or 10 μ M pomalidomide for 7 h, and then lysed with Pierce IP Lysis Buffer (ThermoFisher Scientific) containing 10 mM N-ethylmaleimide (ThermoFisher Scientific), 10 μ M PR-619 (Nacalai Tesque), 10 μ M MG132 (Peptide Institute), and protease/phosphatase inhibitor cocktail. Ubiquitinated proteins were pulled down by incubating lysates with Ubiquitin 1 tandem UBA (TUBE2) agarose (Boston Biochem) for 2 h at 4 °C and washing the beads 3 times with IP lysis buffer. Bound proteins were eluted by incubating the beads with Sample Buffer Solution

with Reducing Reagent (6×) for SDS-PAGE (Nacalai Tesque) at 95 °C for 5 min and separated by SDS-PAGE, followed by immunoblotting using antibodies against PLZF, SALL4, and Ubiquitin.

In vitro ubiquitination assay. Flag-tagged recombinant PLZF (Active Motif) and recombinant CRL4^{CRBN} complex were pre-incubated with DMSO or 100 μM pomalidomide in 1× E3 Ligase Reaction Buffer (R&D Systems) for 30 min at 30 °C. The reactions were then incubated with 100 nM UBE1 (E1; R&D Systems), 500 nM UBE2D3 (E2; R&D Systems), 500 nM UBE2G1 (E2; R&D Systems), 25 μM ubiquitin (R&D Systems), and 2 μM ubiquitin-aldehyde (R&D Systems) in the presence or absence of 1 mM Mg-ATP (R&D Systems) for 90 min at 30 °C. Flag-PLZF was then isolated using anti-Flag affinity gel (Sigma) and subjected to immunoblotting to visualize ubiquitinated PLZF using an anti-ubiquitin antibody (Enzo Life Science).

Cell proliferation analysis. Cells were plated into a 96-well plate and incubated with Cell Count Reagent SF (Nacalai Tesque) for 1–3 h. Then, relative cell numbers were estimated by measuring the absorbance at 450 and 600 nm.

Statistics and reproducibility. Quantitative data were expressed in bar graphs or scatter plots as mean ± standard error of the mean (SEM). The number of tests carried out is stated in figure legends. The data were calculated and analyzed by Microsoft Excel (Microsoft), Prism 8 (GraphPad Software).

Reporting summary. Further information on research design is available in the Nature Research Reporting Summary linked to this article.

Data availability

All data generated or analyzed during this study are included in this published article (and its Supplementary Information files) or are available from the corresponding author on reasonable request. The source data underlying the graphs and charts in the figure are shown in Supplementary Data 2. Proteomics raw data are deposited in the Japan Proteome Standard Repository/Database (jPOST), a member of the ProteomeXchange consortium. The accession numbers are PXD023928 for ProteomeXchange and JPST001075 for jPOST.

Received: 29 December 2020; Accepted: 22 October 2021;

Published online: 11 November 2021

References

- Bartlett, J. B., Dredge, K. & Dalgleish, A. G. The evolution of thalidomide and its IMiD derivatives as anticancer agents. *Nat. Rev. Cancer* **4**, 314–322 (2004).
- Adams, J. et al. Potent and selective inhibitors of the proteasome: dipeptidyl boronic acids. *Bioorg. Med. Chem. Lett.* **8**, 333–338 (1998).
- Ito, T. & Handa, H. Molecular mechanisms of thalidomide and its derivatives. *Proc. Jpn Acad. Ser. B Phys. Biol. Sci.* **96**, 189–203 (2020).
- Singhal, S. et al. Antitumor activity of thalidomide in refractory multiple myeloma. *N. Engl. J. Med.* **341**, 1565–1571 (1999).
- Ito, T. et al. Identification of a primary target of thalidomide teratogenicity. *Science* **327**, 1345–1350 (2010).
- Ito, T. & Handa, H. Myeloid disease: another action of a thalidomide derivative. *Nature* **523**, 167–168 (2015).
- Lu, G. et al. The myeloma drug lenalidomide promotes the cereblon-dependent destruction of Ikaros proteins. *Science* **343**, 305–309 (2014).
- Kronke, J. et al. Lenalidomide causes selective degradation of IKZF1 and IKZF3 in multiple myeloma cells. *Science* **343**, 301–305 (2014).
- Gandhi, A. K. et al. Immunomodulatory agents lenalidomide and pomalidomide co-stimulate T cells by inducing degradation of T cell repressors Ikaros and Aiolos via modulation of the E3 ubiquitin ligase complex CRL4(CRBN). *Br. J. Haematol.* **164**, 811–821 (2014).
- Kronke, J. et al. Lenalidomide induces ubiquitination and degradation of CK1alpha in del(5q) MDS. *Nature* **523**, 183–188 (2015).
- Yamamoto, J. et al. ARID2 is a pomalidomide-dependent CRL4(CRBN) substrate in multiple myeloma cells. *Nat. Chem. Biol.* **16**, 1208–1217 (2020).
- Asatsuma-Okumura, T. et al. p63 is a cereblon substrate involved in thalidomide teratogenicity. *Nat. Chem. Biol.* **15**, 1077–1084 (2019).
- Donovan, K. A. et al. Thalidomide promotes degradation of SALL4, a transcription factor implicated in Duane Radial Ray syndrome. *Elife* **7**, 38430 (2018).
- Matyskiela, M. E. et al. SALL4 mediates teratogenicity as a thalidomide-dependent cereblon substrate. *Nat. Chem. Biol.* **14**, 981–987 (2018).
- Belair, D. G. et al. Thalidomide inhibits human iPSC mesoderm differentiation by modulating CRBN-dependent degradation of SALL4. *Sci. Rep.* **10**, 2864 (2020).
- Matyskiela, M. E. et al. A novel cereblon modulator recruits GSPT1 to the CRL4(CRBN) ubiquitin ligase. *Nature* **535**, 252–257 (2016).
- Petzold, G., Fischer, E. S. & Thoma, N. H. Structural basis of lenalidomide-induced CK1alpha degradation by the CRL4(CRBN) ubiquitin ligase. *Nature* **532**, 127–130 (2016).
- Sievers, Q. L. et al. Defining the human C2H2 zinc finger degrome targeted by thalidomide analogs through CRBN. *Science* **362**, 0572 (2018).
- Matyskiela, M. E. et al. Crystal structure of the SALL4-pomalidomide-cereblon-DDB1 complex. *Nat. Struct. Mol. Biol.* **27**, 319–322 (2020).
- Tan, X. et al. Mechanism of auxin perception by the TIR1 ubiquitin ligase. *Nature* **446**, 640–645 (2007).
- List, A. et al. Lenalidomide in the myelodysplastic syndrome with chromosome 5q deletion. *N. Engl. J. Med.* **355**, 1456–1465 (2006).
- Habermann, T. M. et al. Lenalidomide oral monotherapy produces a high response rate in patients with relapsed or refractory mantle cell lymphoma. *Br. J. Haematol.* **145**, 344–349 (2009).
- Ramsay, A. G. et al. Follicular lymphoma cells induce T-cell immunologic synapse dysfunction that can be repaired with lenalidomide: implications for the tumor microenvironment and immunotherapy. *Blood* **114**, 4713–4720 (2009).
- Rychak, E. et al. Pomalidomide in combination with dexamethasone results in synergistic anti-tumour responses in pre-clinical models of lenalidomide-resistant multiple myeloma. *Br. J. Haematol.* **172**, 889–901 (2016).
- Melnick, A. & Licht, J. D. Deconstructing a disease: RARalpha, its fusion partners, and their roles in the pathogenesis of acute promyelocytic leukemia. *Blood* **93**, 3167–3215 (1999).
- Chen, B. et al. Identification of fusion genes and characterization of transcriptome features in T-cell acute lymphoblastic leukemia. *Proc. Natl Acad. Sci. USA* **115**, 373–378 (2018).
- An, J. et al. pSILAC mass spectrometry reveals ZFP91 as IMiD-dependent substrate of the CRL4(CRBN) ubiquitin ligase. *Nat. Commun.* **8**, 15398 (2017).
- Davies, F. & Baz, R. Lenalidomide mode of action: linking bench and clinical findings. *Blood Rev. Suppl* **1**, S13–S19 (2010).
- Ahmad, K. F., Engel, C. K. & Prive, G. G. Crystal structure of the BTB domain from PLZF. *Proc. Natl Acad. Sci. USA* **95**, 12123–12128 (1998).
- Cook, M. et al. Expression of the zinc-finger gene PLZF at rhombomere boundaries in the vertebrate hindbrain. *Proc. Natl Acad. Sci. USA* **92**, 2249–2253 (1995).
- Costoya, J. A. et al. Essential role of Plzf in maintenance of spermatogonial stem cells. *Nat. Genet.* **36**, 653–659 (2004).
- Kovalovsky, D. et al. The BTB-zinc finger transcriptional regulator PLZF controls the development of invariant natural killer T cell effector functions. *Nat. Immunol.* **9**, 1055–1064 (2008).
- Chen, Z. et al. Fusion between a novel Kruppel-like zinc finger gene and the retinoic acid receptor-alpha locus due to a variant t(11;17) translocation associated with acute promyelocytic leukaemia. *EMBO J.* **12**, 1161–1167 (1993).
- Muller, C. et al. The aberrant fusion proteins PML-RAR alpha and PLZF-RAR alpha contribute to the overexpression of cyclin A1 in acute promyelocytic leukemia. *Blood* **96**, 3894–3899 (2000).
- Rice, K. L. et al. Comprehensive genomic screens identify a role for PLZF-RARalpha as a positive regulator of cell proliferation via direct regulation of c-MYC. *Blood* **114**, 5499–5511 (2009).
- Ruthardt, M. et al. The acute promyelocytic leukaemia specific PML and PLZF proteins localize to adjacent and functionally distinct nuclear bodies. *Oncogene* **16**, 1945–1953 (1998).
- Wang, X., Wang, J. & Zhang, L. Characterization of atypical acute promyelocytic leukaemia: Three cases report and literature review. *Medicine* **98**, e15537 (2019).
- Smith, Z. A., Buchanan, C. C., Raphael, D. & Khoo, L. T. Ossification of the posterior longitudinal ligament: pathogenesis, management, and current surgical approaches. A review. *Neurosurg. Focus* **30**, 10256 (2011).
- Ikedo, R. et al. The promyelocytic leukemia zinc finger promotes osteoblastic differentiation of human mesenchymal stem cells as an upstream regulator of CBFA1. *J. Biol. Chem.* **280**, 8523–8530 (2005).
- Agrawal Singh, S. et al. PLZF targets developmental enhancers for activation during osteogenic differentiation of human mesenchymal stem cells. *Elife* **8**, 40364 (2019).
- Liska, F. et al. Plzf as a candidate gene predisposing the spontaneously hypertensive rat to hypertension, left ventricular hypertrophy, and interstitial fibrosis. *Am. J. Hypertens.* **27**, 99–106 (2014).
- Liska, F. et al. Downregulation of Plzf gene ameliorates metabolic and cardiac traits in the spontaneously hypertensive rat. *Hypertension* **69**, 1084–1091 (2017).

43. Wang, N. et al. Promyelocytic leukemia zinc finger protein activates GATA4 transcription and mediates cardiac hypertrophic signaling from angiotensin II receptor 2. *PLoS ONE* **7**, 35632 (2012).
44. Yamanaka, S. et al. Thalidomide and its metabolite 5-hydroxythalidomide induce teratogenicity via the cereblon neosubstrate PLZF. *EMBO J.* **40**, 105375 (2021).
45. Druker, B. J. et al. Effects of a selective inhibitor of the Abl tyrosine kinase on the growth of Bcr-Abl positive cells. *Nat. Med.* **2**, 561–566 (1996).
46. Dang, C. V., Reddy, E. P., Shokat, K. M. & Soucek, L. Drugging the ‘undruggable’ cancer targets. *Nat. Rev. Cancer* **17**, 502–508 (2017).
47. Lai, A. C. & Crews, C. M. Induced protein degradation: an emerging drug discovery paradigm. *Nat. Rev. Drug Discov.* **16**, 101–114 (2017).
48. Fionda, C. et al. The IMiDs targets IKZF-1/3 and IRF4 as novel negative regulators of NK cell-activating ligands expression in multiple myeloma. *Oncotarget* **6**, 23609–23630 (2015).
49. Maher, C. A. et al. Transcriptome sequencing to detect gene fusions in cancer. *Nature* **458**, 97–101 (2009).
50. Girardi, T., Vicente, C., Cools, J. & De Keersmaecker, K. The genetics and molecular biology of T-ALL. *Blood* **129**, 1113–1123 (2017).
51. Lopez-Girona, A. et al. Cereblon is a direct protein target for immunomodulatory and antiproliferative activities of lenalidomide and pomalidomide. *Leukemia* **26**, 2326–2335 (2012).

Acknowledgements

We thank Kei Taneda, Marika Sato, and Yuka Natori for technical assistance. We thank Profs. Hideyuki Okano and Hironobu Okuno (Department of Physiology, Keio University, Japan) and Prof. Austin Smith (Department of Biochemistry, Cambridge University, UK) for providing It-NES and Sai2, respectively. We also thank Prof. Estelle Duprez (Cancer Research Center of Marseille, France) for providing B412 cells. This work was supported by MEXT/JSPS KAKENHI Grant Numbers 19K16378 (to N.S.), 20K16314 (to T.A.-O.), 20K08741 (to J.Y.), 17H06112 (to H.H. and Y.Y.), 18H05502 (to T.I.) and 21H02955 (to T.I.).

Author contributions

N.S. performed most biochemical experiments corresponding to Figs. 1–5, Supplementary Figs. 1–5. T.A.-O. performed biochemical experiments corresponding to Fig. 1 and Supplementary Fig. 4c. J.Y. performed biochemical experiments corresponding to Fig. 5b and Supplementary Fig. 3e. T.I. performed biochemical experiments corresponding to Fig. 3e and Supplementary Figs. 1b, 2a, and 4c. N.S., T.A.-O., Y.Y., H.H. and T.I.

interpreted all data. N.S., Y.Y. and T.I. wrote the manuscript. N.S. and T.I. planned this study. H.H. and T.I. supervised the project. All authors discussed the results and approved the manuscript.

Competing interests

H.H. has received research support from Bristol Myers Squibb. The remaining authors declare no competing interests.

Additional information

Supplementary information The online version contains supplementary material available at <https://doi.org/10.1038/s42003-021-02801-y>.

Correspondence and requests for materials should be addressed to Hiroshi Handa or Takumi Ito.

Peer review information *Communications Biology* thanks the anonymous reviewers for their contribution to the peer review of this work. Primary Handling Editor: Eve Rogers.

Reprints and permission information is available at <http://www.nature.com/reprints>

Publisher’s note Springer Nature remains neutral with regard to jurisdictional claims in published maps and institutional affiliations.



Open Access This article is licensed under a Creative Commons Attribution 4.0 International License, which permits use, sharing, adaptation, distribution and reproduction in any medium or format, as long as you give appropriate credit to the original author(s) and the source, provide a link to the Creative Commons license, and indicate if changes were made. The images or other third party material in this article are included in the article’s Creative Commons license, unless indicated otherwise in a credit line to the material. If material is not included in the article’s Creative Commons license and your intended use is not permitted by statutory regulation or exceeds the permitted use, you will need to obtain permission directly from the copyright holder. To view a copy of this license, visit <http://creativecommons.org/licenses/by/4.0/>.

© The Author(s) 2021